JOURNAL OF BACTERIOLOGY, July 2010, p. 3801–3808 Vol. 192, No. 14
0021-9193/10/$12.00 doi:10.1128/JB.00117-10

Cochaperone Interactions in Export of the Type III Needle Component PscF of *Pseudomonas aeruginosa*▽

Sophie Plé,[1,2,3] Viviana Job,[4] Andréa Dessen,[4] and Ina Attree[1,2,3]*

UMR 5092, Centre National de la Recherche Scientifique (CNRS),[1] LBBSI, iRTSV, Commissariat à l'Energie Atomique (CEA),[2] Université Joseph Fourier (UJF),[3] and Bacterial Pathogenesis Group, Institut de Biologie Structurale UMR 5075 (CNRS/CEA/UJF),[4] Grenoble, France

Received 2 February 2010/Accepted 15 May 2010

Type III secretion (T3S) systems allow the export and translocation of bacterial effectors into the host cell cytoplasm. Secretion is accomplished by an 80-nm-long needle-like structure composed, in *Pseudomonas aeruginosa*, of the polymerized form of a 7-kDa protein, PscF. Two proteins, PscG and PscE, stabilize PscF within the bacterial cell before its export and polymerization. In this work we screened the 1,320-Å² interface between the two chaperones, PscE and PscG, by site-directed mutagenesis and determined hot spot regions that are important for T3S function *in vivo* and complex formation *in vitro*. Three amino acids in PscE and five amino acids in PscG, found to be relevant for complex formation, map to the central part of the interacting surface. Stability assays on selected mutants performed both *in vitro* on purified PscE-PscG complexes and *in vivo* on *P. aeruginosa* revealed that PscE is a cochaperone that is essential for the stability of the main chaperone, PscG. Notably, when overexpressed from a bicistronic construct, PscG and PscF compensate for the absence of PscE in cytotoxic *P. aeruginosa*. These results show that all of the information needed for needle protein stabilization and folding, its presentation to the T3 secreton, and its export is present within the sequence of the PscG chaperone.

Many Gram-negative bacteria are endowed with a specialized secretion machinery called the type III secretion (T3S) system (T3SS) that allows a set of bacterial proteins (effectors) to be injected directly into a eukaryotic cell cytoplasm. The effectors carry versatile enzymatic activities and target the main host defense functions, such as phagocytosis (14, 19). The T3S nanomachinery is composed of three main subassemblies: the basal body, the needle, and the translocon (5, 15). The basal body, which is in composition and structure similar to a flagellum base, is embedded within two bacterial membranes and is composed of several protein rings made up of identical subunits with 12-fold symmetry (20, 33). Protruding from the surface and in continuum with the base, the needle is formed by a low-molecular-weight protein that polymerizes into a 50- to 80-nm-long and 8-nm-wide structure whose length is highly regulated (22, 24, 27). It is widely accepted that the secretion of effectors takes place through this 2-nm-wide needle channel and is continued through a three-protein pore complex called the translocon. In related T3S systems of pathogens *Pseudomonas aeruginosa* and *Yersinia* spp., the translocon is composed of one hydrophilic (PcrV and LcrV in *Pseudomonas* and *Yersinia*, respectively) and two hydrophobic (PopB/PopD and YopB/YopD, respectively) proteins, which allow crossing of the host plasma membrane (16, 18, 25).

A highlight of the T3S systems is a class of intrabacterial helper proteins, called chaperones, which are proposed to participate in several steps of substrate stabilization and export. The sequence identity between chaperones is notably low, but they possess common features such as small size (100 to 150 residues) and a tendency toward an acidic pI (26). T3S chaperones have been classified into three categories according to their partners and their modes of interaction. Class I chaperones act as dimers and bind one (class IA) or several (class IB) effectors. Crystal structures of several class IA and IB molecules show that they share a similar 5β/3α fold, the central α helix being responsible for dimerization (3, 34). They act mainly as "bodyguards" preventing their substrates from generating premature or nonspecific interactions with other proteins but are also thought to play a role in secretion. The class II chaperones bind to hydrophobic translocators and keep them in a soluble state (13, 31). SycD of *Yersinia* binds YopB and YopD translocators, while PcrH from *Pseudomonas* is responsible for recognition of PopB and PopD (4, 9, 13, 21). These chaperones display all-helical structures with three tetratricopeptide repeat (TPR) motifs, with a single TPR module being composed of two antiparallel α helices; the overall structure forms a concave substrate-binding groove (4, 21, 23).

The third class consists of chaperones interacting with needle proteins. Until now, they have been documented only in the Ysc/Psc subclass of T3SSs (29, 35, 36). We have previously demonstrated that in *P. aeruginosa*, an opportunistic pathogen, the type III needle component PscF is maintained in its monomeric form within the bacterial cytoplasm by a bimolecular chaperone, PscE-PscG (29, 30). The 2-Å crystal structure of the ternary complex revealed that PscE is a 67-amino-acid protein which folds into three α helices (Ha, Hb, and Hc) and interacts directly only with PscG. PscG is composed of seven α helices (H1 to H7) organized into a TPR-like domain harboring a concave region which binds to the C-terminal helix of PscF (30). The interacting surface between PscG and PscF is essential for needle formation and bacterial cytotoxicity (30).

In this work, we investigate the role of two chaperones in

* Corresponding author. Mailing address: LBBSI/iRTSV, CEA-Grenoble, 17 rue des Martyrs, 38054 Grenoble cedex 9, France. Phone: 33 438783483. Fax: 33 438784499. E-mail: iattreedelic@cea.fr.

▽ Published ahead of print on 21 May 2010.

needle protein stabilization and T3S function. We define interaction hot spots of the PscE-PscG surface by site-directed mutagenesis and then show that PscE is required for stabilization of PscG both *in vivo* and *in vitro*. Moreover, we show that when PscG is overproduced in concert with PscF in *P. aeruginosa*, the absence of PscE does not affect T3S functionality. These data demonstrate that PscG is the main needle chaperone, being sufficient to maintain PscF in a secretion-prone fold, and that PscE is a cochaperone needed to ensure stability of PscG.

MATERIALS AND METHODS

***P. aeruginosa* strains.** Construction of *P. aeruginosa* CHA ΔPscE and ΔPscG strains was described previously, as well as the generation of complementing plasmids (29, 30). All tested strains were obtained by complementing the deletion mutants with appropriate plasmids.

Site-directed mutagenesis and cloning. For *in vivo* assays, site-directed mutagenesis was performed on pIApG/*pscE* and pIApG/*pscG* plasmids (29). The bicistronic construct pIApG/*pscF-pscG* was obtained by cloning of the *pscF-pscG* PCR-amplified fragment into pIApG. DNA fragments encoding defined helices of PscE (Ha-Hb, Hb-Hc, and Hc) were obtained by PCR, sequenced, and cloned in pIApG/*pscE* by replacing the wild-type *pscE* fragment. The list of PCR primers is available on request. For *in vitro* complex formation, mutagenesis was performed on pETDuet/*6his-pscE-pscG*. This plasmid was constructed as follows. *pscE* and *pscG* were amplified by PCR and cloned in the vector pETDuet-1 (Novagen). The BamHI/HindIII fragment with the full-length *pscE* was cloned in the first multiple cloning site (MCS), and a thrombin site was added by PCR at the N-terminal end, in order to be able to cleave the 6His tag. The NdeI/XhoI fragment containing the *pscG* gene was cloned in the second MCS. All final constructs were checked by DNA sequencing.

T3S-dependent secretion and cytotoxicity assays. Mutant and control strains were grown on *Pseudomonas* isolation agar (PIA; Difco) plates or in liquid Luria broth (LB) at 37°C with agitation. Carbenicillin was used at 500 μg/ml for PIA plates and 300 μg/ml in LB. For induction of T3S *in vitro*, *P. aeruginosa* overnight cultures were diluted to an optical density at 600 nm (A_{600}) of 0.1 in 30 ml LB containing 5 mM EGTA and 20 mM $MgCl_2$. Incubation was performed for an additional 3 h until the cultures reached A_{600} values of 1.0. The cultures were centrifuged (6,000 rpm, 10 min), and the supernatants were directly analyzed by Western blotting (15 μl used for $A_{600} = 1.0$) using anti-PopB antibodies (17). For cytotoxicity assays, the bacteria were cultivated to an A_{600} of 1.0 and added to macrophage cell line J774 at a multiplicity of infection (MOI) of 5. Cell death was assessed at 3 h postinfection by using a cytotoxicity detection kit (lactate dehydrogenase [LDH]; Roche), as described previously (6). All tests were performed in triplicate.

Protein stability assays. The *P. aeruginosa* overnight cultures were diluted to an A_{600} of 0.1 in 100 ml LB containing 5 mM EGTA and 20 mM $MgCl_2$. Incubation was performed for an additional 3 h until the cultures reached an A_{600} of 1.0, at which point chloramphenicol (500 μg/ml) was added. Samples (4 ml) were taken every 30 min as indicated; centrifuged; resuspended in 80 μl of 25 mM Tris-HCl, 20 mM NaCl, pH 8.0; sonicated; and recentrifuged (13,000 rpm, 10 min). The protein concentration (determined by Coomassie blue protein assay; Pierce) was adjusted, and 50-ng samples were loaded on 18% SDS-PAGE gels and analyzed by immunoblotting with anti-PscG or anti-PscE antibodies.

PscE-PscG complex production and purification. Wild-type PscE-PscG complex and mutant proteins were produced from pETDuet/*6his-pscE-pscG* in *Escherichia coli* BL21(DE3). The overnight cultures were diluted to an A_{600} of 0.1 in 500 ml LB containing ampicillin at 100 μg/ml. Expression was induced with IPTG (isopropyl-β-D-thiogalactopyranoside; 1 mM) for 3 h at 37°C. Cultures were centrifuged (6,000 rpm, 10 min) and resuspended in 20 ml of 25 mM Tris-HCl, 500 mM NaCl, pH 8.0, 2% (vol/vol) glycerol, and 5 mM imidazole supplemented with protease inhibitor cocktail (Complete; Roche). The bacterial suspensions were then broken by using a French pressure cell. After ultracentrifugation, the supernatant was loaded onto a Ni^{2+} affinity column (HiTrap Chelating HP; 1 ml; GE Healthcare) and eluted using increasing imidazole concentrations (from 5 to 200 mM imidazole). For some samples, 300 μl of 150 mM imidazole fractions eluted from a Ni^{2+} column was further analyzed by high-resolution size-exclusion chromatography (SEC; Superdex 200 10/300 GL; GE Healthcare). Column calibration was performed by employing GE Healthcare molecular weight standards. The samples were separated in 25 mM Tris-HCl, 100 mM NaCl, pH 8.0, with a flow rate of 0.5 ml/min.

Antibodies and immunoblot analysis. Polyclonal antibodies against PopB and PscF used in this work were previously described (17, 27). Anti-PscE and anti-PscG were raised in guinea pigs by Eurogentec as described by the manufacturer. Antigens were obtained as described previously (29). All antibodies were affinity purified, using activated CH Sepharose 4B (GE Healthcare) following the manufacturer's instructions. The protein samples were subjected to SDS-PAGE and transferred to nitrocellulose membranes. The membranes were blocked with 5% nonfat dry milk before addition of primary antibodies using dilutions of 1:500 for anti-PscF, 1:3,000 for anti-PopB, 1:2,000 for anti-PscE, and 1:500 for anti-PscG. Secondary goat anti-rabbit (Sigma) or rabbit anti-guinea pig (Invitrogen) antibodies (1:5,000) conjugated to horseradish peroxidase were used. Detection was performed by enhanced chemiluminescence (ECL; GE Healthcare).

RESULTS

Regions of the PscE-PscG interface essential for T3S function. The PscE-PscG interaction surface encompasses an area of 1,321 $Å^2$ where the two chaperones bind to each other through multiple hydrophobic interactions (Fig. 1A). Based on the crystal structure of the PscE-PscF-PscG ternary complex (30), 13 and 5 amino acids were chosen to be mutated in PscE and PscG, respectively, in order to evaluate their importance *in vivo* (Table 1). Amino acid changes were generated on plasmids pIApG-*pscE* and pIApG-*pscG*, which are able to complement *P. aeruginosa* ΔE and ΔG strains, respectively (29, 30). Strains were directly screened through a macrophage cytotoxicity test; results reflected the functionality of the T3S needle (6). Surprisingly, out of 16 mutants created in PscE (11 simple mutants, four double mutants, and one triple mutant), which were hypothesized either to destabilize PscE itself by influencing the interactions between its two α helices (Hb-Hc) or to perturb interactions with PscG, only one double mutation (L20S-L24S) showed a slight effect on bacterial cytotoxicity (Fig. 1B and C). However, the complete deletion of the Hb or Hc helix abrogated bacterial cytotoxicity (Table 1), clearly showing its importance in PscE-PscF-PscG complex formation. These results show that simple changes in the PscE sequence do not influence needle assembly and that multiple anchoring points contribute to the stability of the PscE-PscG complex. Further inspection of the PscE-PscG interface pointed to the possible importance of the glycine at position 57 in the ability of Hc to contribute to complex stability. Indeed, when G57 was drastically changed into an aspartate residue, the mutant strain completely lost the capacity to lyse macrophages, indicating the absence of a functional T3SS.

Out of 12 PscG mutants, one triple mutant and three double mutants were found to display significantly diminished cytotoxicity. These changes map to PscG α helices H1 (L5, L9, and L12) and H2 (I28 and W31) and are in proximity to amino acids L20, L24, and G57 of PscE in helices Hb and Hc (Fig. 1C). All selected mutants were then further analyzed for their capacity to secrete T3S translocator protein *in vitro*. As predicted from the cytotoxicity assays, simple mutants (with the exception of the drastic G57D mutant) exerted no obvious effect on secretion of the translocator PopB, whereas one double (I28S-W31S) and one triple (L9S-I28S-W31S) PscG mutant showed no detectable levels of PopB in culture supernatants (Fig. 1B). All mutations identified by this screen map in the central part of the interacting surface.

The PscE-PscG complex is destabilized by specific mutations. To further determine the importance of the mutations

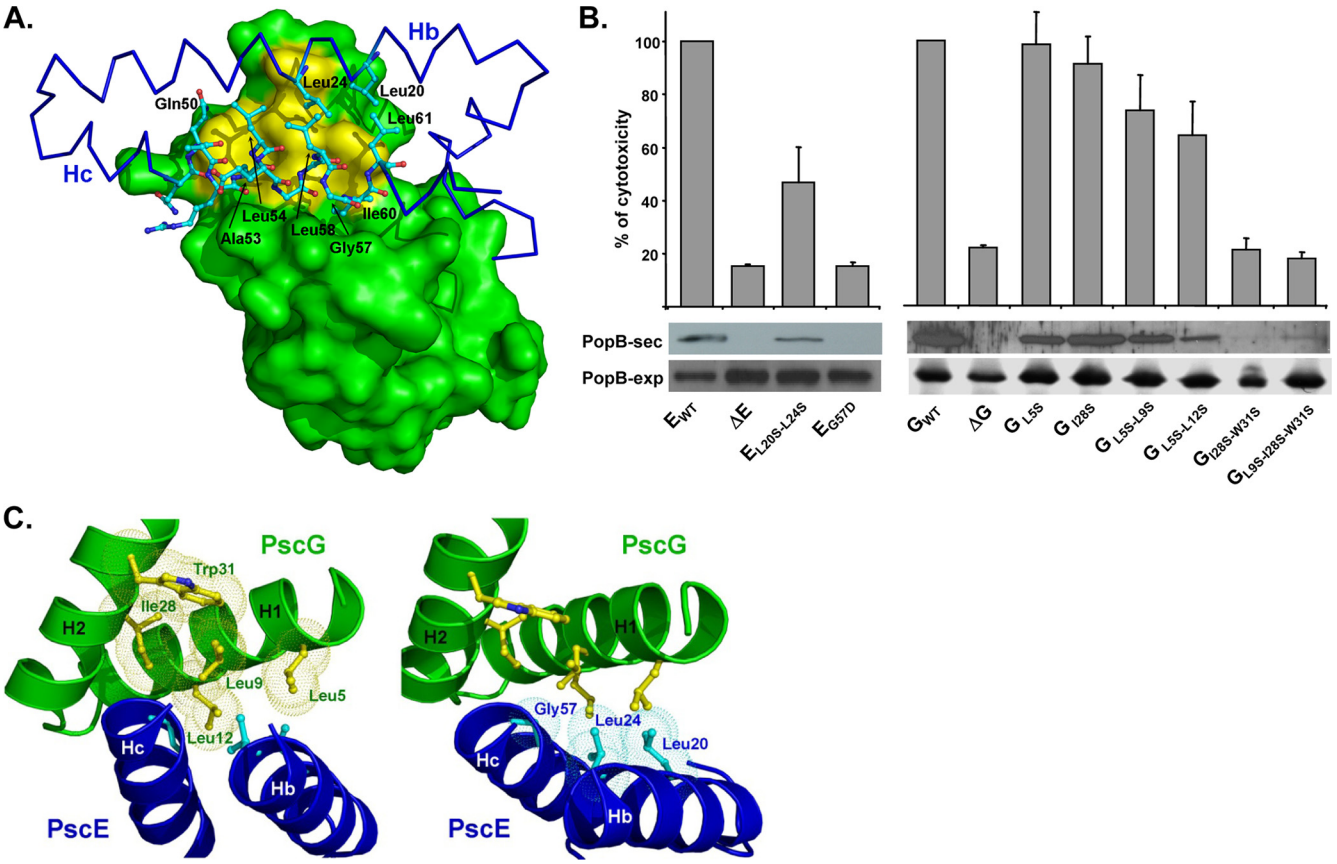

FIG. 1. Screen for essential amino acids within the PscE-PscG interface (also Table 1). (A) PscE-PscG interface showing the relevant amino acids in PscG (green) and PscE (blue). Amino acids L5, L9, L12, I28, and W31 in PscG are highlighted in yellow. The PscE residues are shown as cyan sticks. (B) Cytotoxicity tests on macrophages and T3S-dependent secretion of PopB assayed with selected PscG and PscE mutants. Cytotoxicity assays were performed with a J774 macrophage cell line infected with indicated *P. aeruginosa* strains. Strains used as positive values were the ΔPscG/*pscG* (G_{WT}) and ΔPscE/*pscE* (E_{WT}) strains. Strains used as negative values were the ΔPscG (ΔG) and ΔPscE (ΔE) strains. The secretion (PopB-sec) and expression (PopB-exp) of translocator protein PopB were evaluated by immunoblotting. Bars represent standard deviations. (C) Details of the PscG-PscE interface showing relevant helices H1 and H2 of PscG and Hb and Hc of PscE. Figures in panels A and C were generated with Pymol (http://www.pymol.org).

for complex formation and/or stability, we performed *in vitro* copurifications with selected mutant proteins. PscE and PscG were thus coproduced in *E. coli* from the pETDuet/*6his-pscE-pscG* plasmid and purified by affinity chromatography by taking advantage of the hexahistidine tag on PscE. Some fractions were further analyzed by size-exclusion chromatography (SEC). Purifications were followed by automated protein detection and confirmed by immunoblotting (Fig. 2). Wild-type 6His-PscE and PscG coeluted from a Ni^{2+} affinity column and eluted as a single peak at 16.7 ml from SEC, between protein standards ovalbumin (43 kDa) and RNase A (13.7 kDa), which could correspond to one molecule of 6His-PscE (9.5 kDa) in complex with one molecule of PscG (12.5 kDa) (29; also see Materials and Methods). The drastic G57D mutation within 6His-PscE completely abolished complex formation, with PscG being detected in the flowthrough and wash fractions of the Ni^{2+} affinity column (Fig. 2A). Two previously described mutations, single L20S (which showed no altered cytotoxicity) and double L20S-L24S (cytotoxicity diminished by 40 to 50%), were also recreated within 6His-PscE, in order to evaluate their impact on complex formation. Notably, even the simple L20S mutation showed an altered protein elution profile from the affinity column. When a 150 mM imidazole-eluted fraction was further analyzed by SEC, a small change in the elution profile could be observed with an additional protein peak appearing at 8 ml (corresponding to a protein of >2,000 kDa), suggesting aggregation of at least one of the partners. Indeed, immunoblotting analysis of the fractions from SEC showed that the 8-ml peak contained only the PscG protein. The same was observed with the L20S-L24S double mutation (data not shown). Five mutations were recreated within the PscG protein, L5S, L9S, I28S, L5S-L9S, and I28S-W31S. In all five cases the elution profiles of PscG from Ni^{2+} affinity columns changed, with most of the protein eluting from the column in the flowthrough fractions and at lower concentrations of imidazole compared to the wild-type complex. Notably, when 150 mM imidazole-eluted fractions were analyzed by SEC, in all analyzed samples the PscG protein could be detected in 8-ml fractions (Fig. 2B and data not shown).

Therefore, we conclude that the maintenance of the stability of the PscE-PscG complex depends on the central region of the interface involving, notably, interactions between amino acids

TABLE 1. Cytotoxicity of *P. aeruginosa* strains carrying indicated mutations[a]

Mutant	% Cytotoxicity (mean ± SD)
pscE mutants	
Δ*pscE*	15.1 ± 0.1
$pscE_{Ha\text{-}Hb}$	15.8 ± 0.9
$pscE_{Hb\text{-}Hc}$	86.2 ± 6.3
$pscE_{Hc}$	15.9 ± 1.1
$pscE_{L20S}$	83.9 ± 9.4
$pscE_{L24S}$	89.2 ± 12.2
$pscE_{L28S}$	90.2 ± 9.3
$pscE_{R32A}$	100 ± 8.7
$pscE_{L35S}$	93.3 ± 11.1
$pscE_{Q50A}$	92.8 ± 6.7
$pscE_{A53S}$	89.4 ± 8.3
$pscE_{L54S}$	92.2 ± 12.2
$pscE_{L58S}$	99.6 ± 15.3
$pscE_{I60S}$	86.9 ± 12.2
$pscE_{L61S}$	95.0 ± 7.2
$pscE_{L20S\text{-}L24S}$	46.8 ± 13.4
$pscE_{Q50A\text{-}L54S}$	93.1 ± 1.6
$pscE_{A53S\text{-}L54S}$	90.9 ± 6.7
$pscE_{L58S\text{-}L64S}$	96.0 ± 2.9
$pscE_{Q50A\text{-}A53S\text{-}L54S}$	87.9 ± 3.7
$pscE_{G57D}$	15.3 ± 1.4
pscG mutants	
Δ*pscG*	21.8 ± 1.0
$pscG_{L5S}$	98.6 ± 12.1
$pscG_{L9S}$	91.4 ± 16.6
$pscG_{L12S}$	100 ± 12.3
$pscG_{I28S}$	91.3 ± 10.1
$pscG_{W31S}$	84.4 ± 17.6
$pscG_{L5S\text{-}L9S}$	69.4 ± 13.3
$pscG_{L5S\text{-}L12S}$	72.1 ± 13
$pscG_{L5S\text{-}I28S}$	77.4 ± 4.1
$pscG_{L9S\text{-}I28S}$	44.0 ± 10.3
$pscG_{L9S\text{-}W31S}$	46.1 ± 4.8
$pscG_{I28S\text{-}W31S}$	34.9 ± 4.4
$pscG_{L9SI28S\text{-}W31S}$	17.8 ± 2.4

[a] Cytotoxicity was calculated using ΔPscE/*pscE* and ΔPscG/*pscG* values as 100% values, using J774 macrophages as an infection model, as described in Materials and Methods. All tests were performed in triplicate.

Leu20, Leu24, and Gly57 in PscE and Leu5, Leu9, Leu12, Ile28, and Trp31 in PscG.

The PscE chaperone stabilizes PscG *in vivo*. As mentioned previously, PscE does not interact directly with the needle-forming subunit, PscF. However, a PscE-deficient strain is unable to construct the functional T3S apparatus and thus is noncytotoxic (29). Moreover, the PscG-PscF complex produced in *E. coli* is unstable (29), suggesting that the role of PscE may be to consolidate the PscG-PscF dimer. Indeed, as previously reported (29) for a *pscE*-deleted strain of *P. aeruginosa*, neither PscG nor PscF could be immunodetected. To obtain further insight into the function of these two chaperones, the presence of each protein was first evaluated by Western blotting using *P. aeruginosa* strains carrying the previously selected mutations (Fig. 3A). For $PscG_{L5S}$ and $PscG_{I28S}$ strains, the three proteins PscG, PscE, and PscF were readily detected, at levels similar to those in the wild-type strain. In $PscG_{L5S\text{-}L9S}$ and $PscG_{L5S\text{-}L12S}$ strains, the levels of PscE and PscF were seriously diminished, while in $PscG_{I28S\text{-}W31S}$ and $PscG_{L9S\text{-}I28S\text{-}W31S}$ strains, neither protein could be detected (Fig. 3A). These results are in agreement with our observations concerning complex formation *in vitro*, where PscE-PscG formation is already destabilized with simple and double amino acid changes. Concerning PscE strains, in both $PscE_{L20S\text{-}L24S}$ and $PscE_{G57D}$ mutants, the steady-state levels of PscG and PscF were found to be dramatically affected (Fig. 3A).

To estimate the effects of less pronounced mutations on the stability of PscG, the intracellular stabilities of selected $PscG_{L5S}$ and $PscG_{L5S\text{-}L9S}$ mutants as well as of the $PscE_{G57D}$ strain, used here as a control, were compared to that of the parental wild-type strain. In order to do so, *P. aeruginosa* strains were cultivated under T3S-inducing conditions, and after arrest of protein synthesis by chloramphenicol treatment, protein aliquots were analyzed by immunoblotting. As shown in Fig. 3B, PscG is stable over the 3-h period after protein synthesis arrest in the wild-type background. In the $PscE_{G57D}$ strain, PscG was not detected even at time zero, as expected and in agreement with cytotoxicity data. Notably, two strains ($PscG_{L5S}$ and $PscG_{L5S\text{-}L9S}$) in which the PscG-PscE surface was only slightly disturbed by the mutations and in which the cytotoxicity was diminished by only 10 to 20% compared to the wild type showed degradation of PscG over time, which was more rapid in the double $PscG_{L5S\text{-}L9S}$ mutant (Fig. 3B). Therefore, even small perturbations of the interface between the two chaperones can diminish the stability of the main chaperone PscG and may perturb T3S assembly.

PscG and PscF provided in *trans* compensate for the absence of PscE. From the structure of the ternary complex (30), PscG appears as the main chaperone for PscF, masking its polymerization domain and inhibiting premature fiber formation. Our previous results suggest that the role of PscE is essentially to stabilize the PscF-PscG heterodimer through multiple interactions with the convex side of the PscG chaperone. Therefore, we asked whether PscG could be sufficient for PscF export and needle formation. As PscG alone is unable to complement the *pscE* deletion mutant (Fig. 4), probably due to rapid degradation of endogenous chromosomally encoded PscF, we constructed a bicistronic plasmid that allowed the synthesis of both PscG and PscF. When this plasmid was introduced into a PscE-deficient strain, the intracellular quantities of PscG and PscF were readily detected by Western blotting (Fig. 4A). The *P. aeruginosa* ΔPscE strain supplemented by a PscG-PscF-expressing plasmid recovered the capability to secrete PopB, as well as restoring T3S-dependent cytotoxicity on macrophages to wild-type levels (Fig. 4B). This result clearly demonstrates that when provided in a large quantity, and in concert with its substrate, PscG is able to accomplish all of the functions of the main needle protein chaperone.

DISCUSSION

The trimeric PscE-PscF-PscG complex is unique in its structure and function in type III secretion. PscE, and its homologue YscE in *Yersinia*, folds into three α helices and was predicted previously to be a chaperone of needle components (7, 28), based basically on homology with chaperones of subunits forming other filamentous structures, such as FliC of flagella and *E. coli* T3S EspA (12, 37). However, crystal structures of two trimeric complexes, PscE-PscF-PscG of *P. aeruginosa* and YscE-YscF-YscG of *Yersinia pestis*, clearly showed

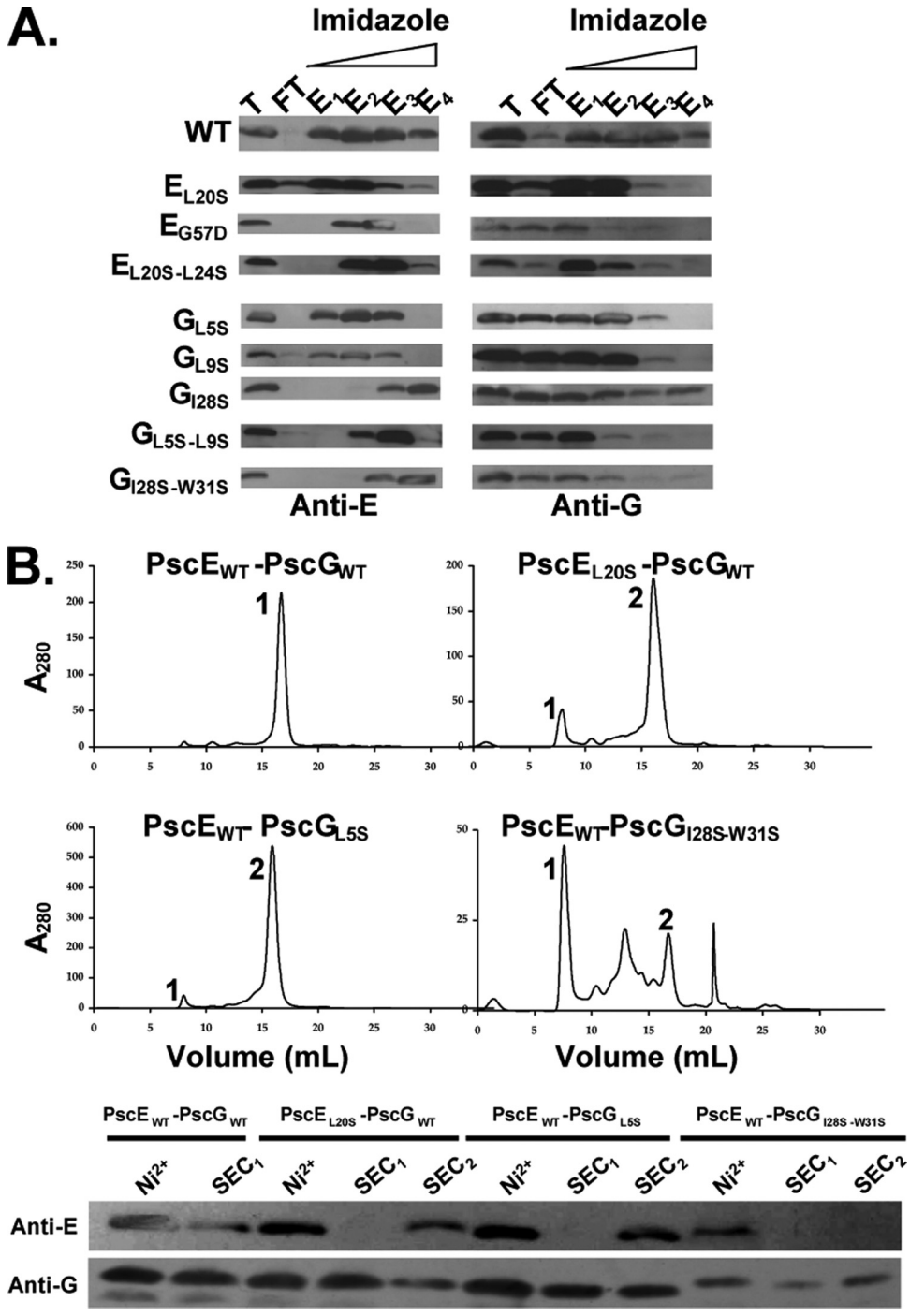

FIG. 2. Formation of mutant PscE-PscG complexes *in vitro*. (A) Selected mutations were recreated in pETDuet/*6his-pscE-pscG*, allowing the production of proteins in *E. coli* BL21(DE3) followed by purification of the 6His-PscE-PscG complexes on Ni^{2+} affinity columns. The presence of PscE and PscG in total cellular extracts (T), flowthrough (FT), and elution fractions (E) obtained by increasing concentrations of imidazole (E1, 100 mM; E2, 150 mM; E3, 200 mM; E4, 250 mM) was confirmed by immunodetection using specific anti-PscE and anti-PscG antibodies. The G57D mutation completely abolished complex formation *in vitro*, while other mutations modified the elution profiles to different extents. (B) Three selected complexes eluted from Ni^{2+} affinity columns in 150 mM imidazole fractions were further analyzed by SEC, and the presence of proteins in different fractions (SEC_1 and SEC_2) was verified by immunoblotting, as in panel A. While the wild-type complex eluted as a single peak at an elution volume of 16 ml, the SEC profiles of mutant complexes showed the appearance of an additional peak at 8 ml, in which the presence of PscG was confirmed using anti-PscG antibodies.

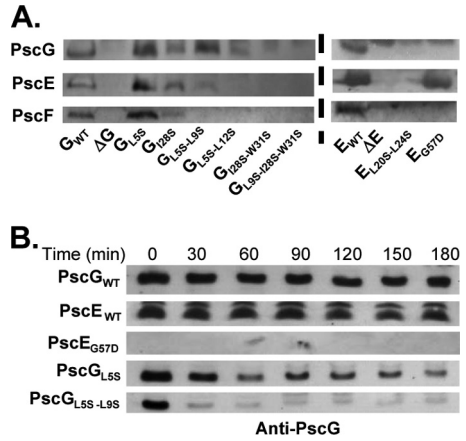

FIG. 3. The stability of PscE and PscG in *P. aeruginosa* depends on their efficient interaction. (A) Whole-cell extracts from *P. aeruginosa* strains carrying mutations described in Fig. 1 were analyzed by Western blotting with antibodies directed toward PscE, PscG, and PscF. (B) Time-lapse stability of PscG in whole-cell extracts after protein arrest induced by chloramphenicol addition at T_0. At indicated time points the same quantity of *P. aeruginosa* cells was withdrawn, sonicated, and analyzed by Western blotting using anti-PscG antibodies. Stabilities of $PscG_{L5S}$ and $PscG_{L5S\text{-}L9S}$ mutants were compared to those of PscG in the parental strain and to the $PscE_{G57D}$ strain, where the complex formation was completely abolished.

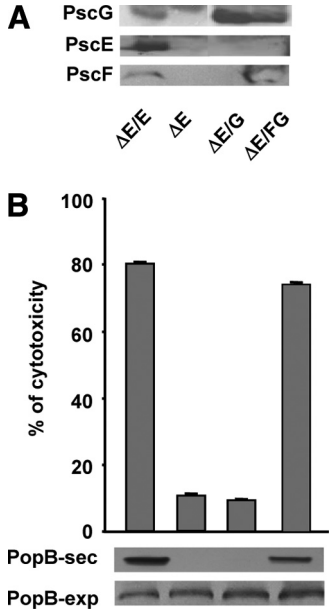

FIG. 4. The PscG chaperone is required and sufficient for PscF export and T3S functionality. (A) A *P. aeruginosa* strain deficient in PscE (ΔE) was supplied in *trans* with either PscG (G) and PscE (E) alone or PscF-PscG (FG) expressed from the bicistronic construct. The presence of proteins was checked by Western blotting using appropriate antibodies. (B) Cytotoxicity assays on macrophages and secretion tests of the PopB translocator performed with the same strains (ΔE/E, ΔE, ΔE/G, and ΔE/FG) as those described for Fig. 1. Note the compensation of T3S function in *P. aeruginosa* ΔPscE when both PscG and PscF were provided.

that PscE/YscE only peripherally contact the needle subunit through the N-terminal α helix, Ha (30, 35). Indeed, the deletion of this helix did not have any effect either on the complex formation *in vitro* or on bacterial cytotoxicity (30). Two additional α helices of PscE (Hb and Hc) extensively interact with each other and with the exterior, convex part of the PscG chaperone, notably with helices H1 and H2. The surface encompassing this interaction is estimated to be >1,300 Å^2 and involves multiple amino acid contacts (30). Our screen of this surface, based on a sensitive cytotoxicity test which reflects T3S function, showed that the central part of the surface is essential for complex stability. Discrete single amino acid changes introduced within PscE and PscG did not perturb the T3S assembly, demonstrating that multiple interactions guarantee complex stability. These experiments clearly demonstrated that the stability of the PscE-PscG complex is maintained throughout the surface by several anchoring points. One drastic mutation in PscE, the change of Gly 57 into Asp, abolished complex formation and was used throughout this work as a negative control. This mutation, created in the central part of the interface, potentially abrogated several interactions around glycine 57 (Fig. 1A). To confirm the results of our *in vivo* screen, we transferred selected mutations into a bicistronic vector which enabled us to coexpress and copurify PscE-PscG complexes *in vitro*. Analyses of mutant complexes by size-exclusion chromatography demonstrated that single and double mutations within PscE and PscG destabilized the complex and one PscG sample aggregated. This finding is in accordance with our observation that, although the PscF-PscG complex could be purified *in vitro* even in the absence of PscF, this binary complex is extremely unstable (29).

As previously suggested by our analysis of PscE- and PscG-deficient mutants in cytotoxic *P. aeruginosa*, the three partners within the trimeric complex costabilize each other; two chaperones are undetectable by Western blotting at steady-state levels in crude extracts of corresponding mutants (29) (Fig. 3). Therefore, to be able to study the action of PscE on the stability of PscG, we selected two mutations whose effects on T3S are detectable neither by the cytotoxicity test nor by the secretion assay. The stability of mutant proteins $PscG_{L5S}$ and $PscG_{L5S\text{-}L9S}$ was evaluated after arrest of protein synthesis and compared with that of PscG in parental strains. Indeed, although the single mutation caused protein stability to decrease, the double mutation had an even more pronounced effect. However, as those mutations had no effect on T3S function as determined by measurements of bacterial cytotoxicity, the intracellular pool of the PscE-PscF-PscG complex should be sufficient for proper export of PscF onto the bacterial surface. Indeed, it was already observed that relatively small amounts of T3S proteins are sufficient to provoke measurable damage on infected macrophages (8).

PscF belongs to the first class of exported substrates of the T3S base, which itself is assembled within the two bacterial membranes by a general secretion pathway. The PscF molecule possesses the intrinsic capacity to polymerize into long fibers, when expressed in a heterologous host; this feature is controlled by the PscE-PscG dimer that ensures the monomeric state of PscF within the bacterial cytoplasm before its transport (30). The structure of PscG harbors three TPR motifs with seven α helices, three of which interact directly with the C-terminal helix of PscF. The PscG-PscF interface is essential for

PscF stability, export, and needle formation, as even single mutations within the interface abrogate T3S function (30). The TPR fold of PscG is highly reminiscent of that of class II chaperones of T3S, such as SycD of *Yersinia*, IpgC of *Shigella*, and PcrH of *Pseudomonas*, whose substrates are hydrophobic translocators (4, 21, 23). Curiously, these chaperones do not require any additional protein or sequence to enhance their intrabacterial stability.

The PscE-PscG complex motif is structurally reminiscent of widespread eukaryotic proteins of the 14-3-3 family, which are implicated in cell signaling by interacting with more than 200 partners involved in a broad range of pathways (1). These protein-protein interactions occur through the conserved TPR motifs of 14-3-3 within a bundle of nine α helices. Helices 1 and 2 in 14-3-3, which could structurally correspond to Hb and Hc in PscE, have been shown to be required for functional dimer formation (1). Therefore, it could have been reasonable to postulate that PscE is somehow involved in protein-protein interactions within the T3S base, in order to "promote" the export of the needle subunits. Our work clearly shows that this is not the case. We were able to construct a *P. aeruginosa* strain deficient in PscE that possesses a functional T3S apparatus, by supplying it with several copies of PscG and PscF. This clearly demonstrates that the PscG chaperone harbors all of the information needed for PscF export within its sequence.

The molecular mechanism which dictates the hierarchical export of substrates is still a largely obscure aspect of the T3S. It has been proposed that the T3S-specific ATPase, located at the cytoplasmic side of the secreton, is implicated in substrate export, notably through an ATP-dependent separation of a chaperone-substrate complex (2). Recently, it has been proposed that in *Chlamydia* a multiple cargo secretion chaperone (Mcsc) associates at the same time with an inner ring protein of the T3S base and with the substrate-chaperone complexes, providing a platform for substrate export. However, a direct interaction between Mcsc and the needle-chaperone complex CdsEGF could not be identified in that work (32). Indeed, the general chaperone FliJ in the flagellar T3S system binds the C-ring component FliM and recognizes the subset of chaperones of "late" flagellum components, and not the FliC-chaperone complex (10, 11). The search for partners of the PscG chaperone in the *P. aeruginosa* T3S system is under way and may provide information that is still lacking regarding the interaction network involved in assembly of the T3S nanomachinery.

ACKNOWLEDGMENTS

S.P. was supported by a postdoctoral fellowship from the Direction des Sciences du Vivant (DSV), CEA.

We thank Eric Faudry for helpful suggestions regarding protein purification experiments. Sylvie Elsen is specially thanked for critical reading of the manuscript. I.A. thanks all the members of the Bacterial Pathogenesis and Cellular Responses team for helpful discussions over the period of this work.

REFERENCES

1. **Aitken, A.** 2006. 14-3-3 proteins: a historic overview. Semin. Cancer Biol. **16:**162–172.
2. **Akeda, Y., and J. E. Galan.** 2005. Chaperone release and unfolding of substrates in type III secretion. Nature **437:**911–915.
3. **Birtalan, S. C., R. M. Phillips, and P. Ghosh.** 2002. Three-dimensional secretion signals in chaperone-effector complexes of bacterial pathogens. Mol. Cell **9:**971–980.
4. **Buttner, C. R., I. Sorg, G. R. Cornelis, D. W. Heinz, and H. H. Niemann.** 2008. Structure of the *Yersinia enterocolitica* type III secretion translocator chaperone SycD. J. Mol. Biol. **375:**997–1012.
5. **Cornelis, G. R.** 2006. The type III secretion injectisome. Nat. Rev. Microbiol. **4:**811–825.
6. **Dacheux, D., J. Goure, J. Chabert, Y. Usson, and I. Attree.** 2001. Pore-forming activity of type III system-secreted proteins leads to oncosis of *Pseudomonas aeruginosa*-infected macrophages. Mol. Microbiol. **40:**76–85.
7. **Deane, J. E., P. Roversi, F. S. Cordes, S. Johnson, R. Kenjale, S. Daniell, F. Booy, W. D. Picking, W. L. Picking, A. J. Blocker, and S. M. Lea.** 2006. Molecular model of a type III secretion system needle: implications for host-cell sensing. Proc. Natl. Acad. Sci. U. S. A. **103:**12529–12533.
8. **Edqvist, P. J., M. Aili, J. Liu, and M. S. Francis.** 2007. Minimal YopB and YopD translocator secretion by *Yersinia* is sufficient for Yop-effector delivery into target cells. Microbes Infect. **9:**224–233.
9. **Edqvist, P. J., J. E. Broms, H. J. Betts, A. Forsberg, M. J. Pallen, and M. S. Francis.** 2006. Tetratricopeptide repeats in the type III secretion chaperone, LcrH: their role in substrate binding and secretion. Mol. Microbiol. **59:**31–44.
10. **Evans, L. D., and C. Hughes.** 2009. Selective binding of virulence type III export chaperones by FliJ escort orthologues InvI and YscO. FEMS Microbiol. Lett. **293:**292–297.
11. **Evans, L. D., G. P. Stafford, S. Ahmed, G. M. Fraser, and C. Hughes.** 2006. An escort mechanism for cycling of export chaperones during flagellum assembly. Proc. Natl. Acad. Sci. U. S. A. **103:**17474–17479.
12. **Evdokimov, A. G., J. Phan, J. E. Tropea, K. M. Routzahn, H. K. Peters, M. Pokross, and D. S. Waugh.** 2003. Similar modes of polypeptide recognition by export chaperones in flagellar biosynthesis and type III secretion. Nat. Struct. Biol. **10:**789–793.
13. **Faudry, E., V. Job, A. Dessen, I. Attree, and V. Forge.** 2007. Type III secretion system translocator has a molten globule conformation both in its free and chaperone-bound forms. FEBS J. **274:**3601–3610.
14. **Galan, J. E.** 2009. Common themes in the design and function of bacterial effectors. Cell Host Microbe **5:**571–579.
15. **Galan, J. E., and H. Wolf-Watz.** 2006. Protein delivery into eukaryotic cells by type III secretion machines. Nature **444:**567–573.
16. **Goure, J., P. Broz, O. Attree, G. R. Cornelis, and I. Attree.** 2005. Protective anti-V antibodies inhibit *Pseudomonas* and *Yersinia* translocon assembly within host membranes. J. Infect. Dis. **192:**218–225.
17. **Goure, J., A. Pastor, E. Faudry, J. Chabert, A. Dessen, and I. Attree.** 2004. The V antigen of *Pseudomonas aeruginosa* is required for assembly of the functional PopB/PopD translocation pore in host cell membranes. Infect. Immun. **72:**4741–4750.
18. **Hakansson, S., T. Bergman, J. C. Vanooteghem, G. Cornelis, and H. Wolf-Watz.** 1993. YopB and YopD constitute a novel class of *Yersinia* Yop proteins. Infect. Immun. **61:**71–80.
19. **Hauser, A. R.** 2009. The type III secretion system of *Pseudomonas aeruginosa*: infection by injection. Nat. Rev. Microbiol. **7:**654–665.
20. **Hodgkinson, J. L., A. Horsley, D. Stabat, M. Simon, S. Johnson, P. C. da Fonseca, E. P. Morris, J. S. Wall, S. M. Lea, and A. J. Blocker.** 2009. Three-dimensional reconstruction of the *Shigella* T3SS transmembrane regions reveals 12-fold symmetry and novel features throughout. Nat. Struct. Mol. Biol. **16:**477–485.
21. **Job, V., P. J. Mattei, D. Lemaire, I. Attree, and A. Dessen.** 12 April 2010, posting date. Structural basis of chaperone recognition of type III secretion system minor translocator proteins. J. Biol. Chem. [Epub ahead of print.] doi:10.1074/jbc.M110.111278.
22. **Journet, L., C. Agrain, P. Broz, and G. R. Cornelis.** 2003. The needle length of bacterial injectisomes is determined by a molecular ruler. Science **302:**1757–1760.
23. **Lunelli, M., R. K. Lokareddy, A. Zychlinsky, and M. Kolbe.** 2009. IpaB-IpgC interaction defines binding motif for type III secretion translocator. Proc. Natl. Acad. Sci. U. S. A. **106:**9661–9666.
24. **Mota, L. J., L. Journet, I. Sorg, C. Agrain, and G. R. Cornelis.** 2005. Bacterial injectisomes: needle length does matter. Science **307:**1278.
25. **Mueller, C. A., P. Broz, and G. R. Cornelis.** 2008. The type III secretion system tip complex and translocon. Mol. Microbiol. **68:**1085–1095.
26. **Page, A. L., and C. Parsot.** 2002. Chaperones of the type III secretion pathway: jacks of all trades. Mol. Microbiol. **46:**1–11.
27. **Pastor, A., J. Chabert, M. Louwagie, J. Garin, and I. Attree.** 2005. PscF is a major component of the *Pseudomonas aeruginosa* type III secretion needle. FEMS Microbiol. Lett. **253:**95–101.
28. **Phan, J., B. P. Austin, and D. S. Waugh.** 2005. Crystal structure of the *Yersinia* type III secretion protein YscE. Protein Sci. **14:**2759–2763.
29. **Quinaud, M., J. Chabert, E. Faudry, E. Neumann, D. Lemaire, A. Pastor, S. Elsen, A. Dessen, and I. Attree.** 2005. The PscE-PscF-PscG complex controls type III secretion needle biogenesis in *Pseudomonas aeruginosa*. J. Biol. Chem. **280:**36293–36300.
30. **Quinaud, M., S. Ple, V. Job, C. Contreras-Martel, J. P. Simorre, I. Attree, and A. Dessen.** 2007. Structure of the heterotrimeric complex that regulates type III secretion needle formation. Proc. Natl. Acad. Sci. U. S. A. **104:**7803–7808.
31. **Schoehn, G., A. M. Di Guilmi, D. Lemaire, I. Attree, W. Weissenhorn, and**

A. Dessen. 2003. Oligomerization of type III secretion proteins PopB and PopD precedes pore formation in *Pseudomonas*. EMBO J. **22:**4957–4967.
32. **Spaeth, K. E., Y. S. Chen, and R. H. Valdivia.** 2009. The *Chlamydia* type III secretion system C-ring engages a chaperone-effector protein complex. PLoS Pathog. **5:**e1000579.
33. **Spreter, T., C. K. Yip, S. Sanowar, I. Andre, T. G. Kimbrough, M. Vuckovic, R. A. Pfuetzner, W. Deng, A. C. Yu, B. B. Finlay, D. Baker, S. I. Miller, and N. C. Strynadka.** 2009. A conserved structural motif mediates formation of the periplasmic rings in the type III secretion system. Nat. Struct. Mol. Biol. **16:**468–476.
34. **Stebbins, C. E., and J. E. Galan.** 2001. Maintenance of an unfolded polypeptide by a cognate chaperone in bacterial type III secretion. Nature **414:**77–81.
35. **Sun, P., J. E. Tropea, B. P. Austin, S. Cherry, and D. S. Waugh.** 2008. Structural characterization of the *Yersinia pestis* type III secretion system needle protein YscF in complex with its heterodimeric chaperone YscE/YscG. J. Mol. Biol. **377:**819–830.
36. **Tan, Y. W., H. B. Yu, K. Y. Leung, J. Sivaraman, and Y. K. Mok.** 2008. Structure of AscE and induced burial regions in AscE and AscG upon formation of the chaperone needle-subunit complex of type III secretion system in *Aeromonas hydrophila*. Protein Sci. **17:**1748–1760.
37. **Yip, C. K., B. B. Finlay, and N. C. Strynadka.** 2005. Structural characterization of a type III secretion system filament protein in complex with its chaperone. Nat. Struct. Mol. Biol. **12:**75–81.